

## A Study of the Spectrum of the OH Megamaser in III Zw 35<sup>1</sup>

Zhi-yao Yu

*Shanghai Astronomical Observatory and Union Laboratory of Radio Astronomy, The Chinese Academy of Science, 80 Nandan Road, Shanghai 200030, China*

III Zw 35 is an OH megamaser galaxy which is of great interest. In this paper, the spectrum has been fitted and the position map has been studied. A new model of multiple and distinct rotating and expanding rings in a thin disk is proposed in this paper.

### 1. Single-Dish Observations and Model I

#### 1.1. Fitting the Spectrum

There are two OH peaks in the spectrum observed by Staveley-Smith et al. (1987) with a single-dish receiver: (1) a main peak with heliocentric velocity  $V_{helio} = 8243 \text{ km s}^{-1}$  and flux density  $S = 219 \text{ mJy}$ , and (2) a secondary peak with  $S = 122 \text{ mJy}$  at  $V_{helio} = 8310 \text{ km s}^{-1}$ . We have found that the OH megamaser spectrum can be fitted with the function

$$S(\text{mJy}) = \exp \left[ \frac{1}{3 \times 10^{-5}(V_{helio} - 8243)^2 + 0.185} \right] \quad (1)$$

for the main peak, and

$$S(\text{mJy}) = \exp \left[ \frac{1}{7.5 \times 10^{-5}(V_{helio} - 8310)^2 + 0.20} \right] \quad (2)$$

for the secondary peak, where in both equations  $V_{helio}$  is in units of  $\text{km s}^{-1}$ . The observed spectrum from Staveley-Smith et al. (1987) and the fits of eqs. (1) and (2) are shown in Fig. 1, which shows that the fit is a good description of the data.

#### 1.2. Model and Results

Assume that OH megamaser spots rotate and expand along the radial direction in a narrow-line region (NLR) that we take to be a thin disk which is seen edge on. We assume that the radial motion and tangential (rotational) motion of a spot is described by  $V_r = V_{r0}\rho^\alpha$ ,  $V_t = V_{t0}\rho^\beta$ , where  $\alpha$  and  $\beta$  are free parameters,  $V_r$  and  $V_t$  are the radial expansion and tangential velocities, respectively, at radius  $r$ , and  $V_{r0}$  and  $V_{t0}$  are the radial and tangential velocities, respectively,

---

<sup>1</sup>This work is supported by the National Natural Science Foundation of China.

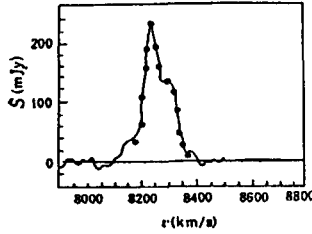


Figure 1. The observational results (solid line) and model fit (dots).

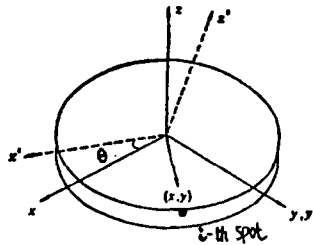


Figure 2. The disk geometry and coordinate systems.

at the radius of a reference point  $r_0$ . We assume that all physical quantities are independent of height in the disk. The pumping rate of the OH megamaser is taken to be constant with radius. In order to further simplify the model and emphasize the kinetic effects, and angular size  $\Omega$  of the OH megamaser spots is assumed to be constant, and the megamaser emission is further assumed to be non-saturated.

In general, the disk will be inclined at some angle  $\theta$  to the line of sight, but megamaser pumping requires a large column density of OH molecules, so we assume that in galaxies in which megamasers are detected that the galaxy is nearly edge-on, i.e.  $\theta = 0$ . The disk geometry and coordinate systems adopted are shown in Fig. 2. The unprimed axes are those appropriate for describing quantities in the plane of the disk, while the primed coordinates are obtained by a rotation by  $\theta$  about the  $y$ -axis, and are more appropriate for the observer's view of the system. The  $x'$  axis is the observer's line of sight, and the  $y'-z'$  plane is the plane of the sky. The gas density has been assumed to be proportional to  $r^\delta$ , where  $\delta$  is an undetermined parameter. We obtain

$$S = P \exp \left[ \frac{1}{a(V_{helio} - V_p)^2 + b} \right], \tag{3}$$

where

$$a = [\alpha r^\delta + 1] [Q \Delta V_{therm} \cos \theta V_{r0}(r/r_0)^\alpha]^{-1},$$

$$V_p = - \left( 1 + \frac{1 - \beta}{2\alpha} \right) \left( \frac{y}{r} \right) \cos \theta V_{t0}(r/r_0)^\beta,$$

and

$$b = a \left[ V_p \left( 1 + \frac{1 - \beta}{2\alpha} \right)^{-1} \right]^2 \left[ \frac{1}{\alpha} (V_{r0}/V_{t0})^2 (r/r_0)^{\alpha - \beta} - \left( \frac{1 - \beta}{2\alpha} \right)^2 \right],$$

where  $S$  is the flux density,  $P = \Omega[I(0) + \epsilon/(-k)]$ , and

$$Q = Bh\nu(n_2 - n_1)/[4\pi\Delta\nu(n_2 + n_1)]$$

is a parameter which depends on the fit. From eq. (3) we can find the fluxes  $S$  corresponding to the peaks of the OH megamaser spectrum. Both the main and secondary peaks of the OH megamaser spectrum may correspond to radiation from different OH megamaser spots at different  $r$  and  $y$ .

The systemic velocity is  $8245 \text{ km s}^{-1}$ , based on optical observations, and is coincident with the velocity of the OH 1667 MHz emission peak (Chapman et al. 1990). In eq. (3), the parameters  $\alpha$ ,  $\beta$ ,  $\delta$ ,  $r_0$ ,  $V_{r0}$ ,  $V_{t0}$ ,  $P$ , and  $\theta$  all are determined by our fit, i.e., eqs. (1) and (2) and our knowledge of OH megamaser galaxies. The choice of parameters is very important, and they must be selected carefully. The choice of the parameters is based on (a) the fit results, (b) comparison of eqs. (1) and (2) with eq. (3), (c) the previous model, and (d) the observational results. Because the OH megamaser galaxy must be edge-on,  $\theta = 0$  (Chapman et al. 1990). We take  $\delta = -3$  following Chevalier & Clegg (1985). Obviously, assuming  $r_0 = 400 \text{ pc}$  is appropriate in general for an OH megamaser galaxy (Baan et al. 1989, Baan 1990). By comparing eq. (3) with eqs. (1) and (2), we find  $P = 1$ . Because the disk-rings are accelerated and spots in rings are rotating, we assume that  $\alpha = 2.5$ ,  $\beta = -2.5$ ,  $V_{r0} = 280 \text{ km s}^{-1}$ , and  $V_{t0} = 70 \text{ km s}^{-1}$  (Harwit et al. 1987, Chevalier & Clegg 1985, Caroll & Kwan 1985, Baan et al. 1989). Our results, which we refer to as Model I, are that  $r = 425 \text{ pc}$ ,  $y = 8 \text{ pc}$ , and  $V(r) = 320 \text{ km s}^{-1}$  for the main peak, and  $r = 322 \text{ pc}$ ,  $y = -106 \text{ pc}$ , and  $V(r) = 159 \text{ km s}^{-1}$  for the secondary peak. The main and second peaks of OH megamaser spectrum of III Zw 35 are formed at different  $r$  and  $y$  in the thin disk. The projected distance in sky plane between the two peaks is  $114 \text{ pc}$  and the difference in radial location is  $103 \text{ pc}$ . Chapman et al. (1990) showed that the OH megamaser of III Zw 35 is distributed within the nuclear region of the galaxy within a linear diameter smaller than  $160 \text{ pc}$ . This was later confirmed by Montgomery & Cohen (1992), who resolved the maser features and found an overall diameter of only  $100 \text{ pc}$ . Our results are consistent with these observations.

## 2. MERLIN Observations and Model II

### 2.1. Selected Data and Basic Theory

III Zw 35 was mapped on 1986 April 27 using four telescopes of the MERLIN network by Montgomery & Cohen (1992). The OH emission centroids shift systematically in position with velocity across the spectrum, tracing out the characteristic signature of a rotating disk. Results for the redshifted 1667 MHz line are plotted in Fig. 3. The disk geometry and adopted coordinate systems are as in Fig. 2.

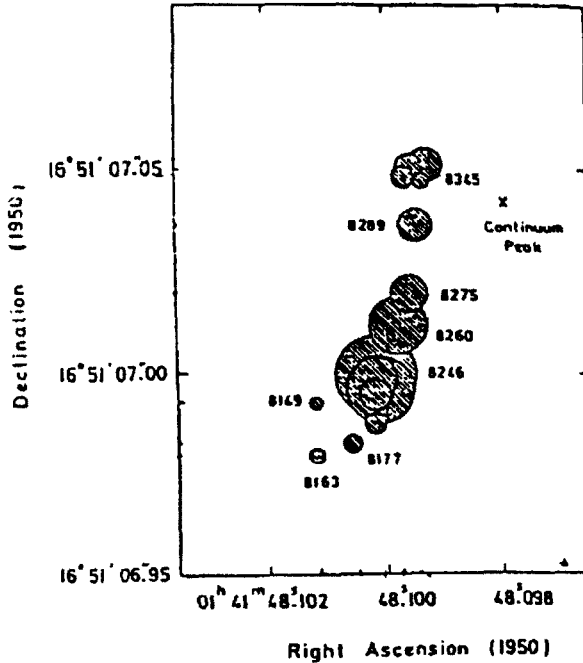


Figure 3. The position map of OH megamaser spots from III Zw 35.

For the  $i$ -th OH megamaser spot in a rotating and expanding ring,  $\rho_i^2 = \rho^2 - (\rho^2/V_e^2)\Psi$ , where  $\Psi = [(V_i - V_0)/(\cos\theta) - \rho_i D\omega]^2$  and  $\rho_i$  is the projected distance of the line linking the  $i$ th spot and the reference point,  $\rho$  is the radius  $r$  of the disk-ring,  $V_e$  is radial velocity at which the disk-ring expands,  $V_i$  is the radial velocity of  $i$ -th spot,  $V_0$  is the systemic velocity of the disk-ring,  $\omega$  is the angular velocity of the disk-ring rotation, and  $D$  is the distance of to III Zw 35. For a specified rotating and expanding disk-ring,  $\rho$ ,  $V_e$ , and  $\omega$  are fixed, as of course, are  $V_0$ ,  $D$ , and  $\theta$ .

We thus introduce a new idea, i.e., multiple distinct rotating and expanding disk-rings. We take the position of the disk-ring center on the position map of OH emission centroids for the redshifted 1667 MHz line in III Zw 35 to be  $\alpha_{1950} = 1^{\text{h}} 41^{\text{m}} 47^{\text{s}}.907$  and  $\delta_{1950} = 16^{\circ} 51' 06''.25$ . We measure the projected distance  $\rho_i$  and corresponding velocity  $V_i$  of every spot, and obtain a locus of  $\rho_i^2$ ,  $\Psi$  values. We find that the distribution of points with coordinate values  $\rho_i^2$  and  $\Psi$  is divided into a few regions. We conclude that OH 1667 MHz maser spots are distributed in a ring in only a few localized regions. By least-squares fitting, we find the values of  $\rho^2$  and  $V_e^2$ , respectively.

## 2.2. Results and Discussion

Our results, which we refer to as 'Model II', are summarized in Table 1.

We summarize our conclusions as follows:

Table 1. Model II Results

Ring	Spots ( $\text{km s}^{-1}$ )	$r$ (pc)	$V_e$ ( $\text{km s}^{-1}$ )
Main peak	8246, 8149, 8177, 8163	447	326
Secondary peak	8345, 8289, 8275, 8260	336	148

1. The OH megamaser spot corresponding to the main peak (i.e., the spot at  $V_{helio} = 8245 \text{ km s}^{-1}$ ) and one corresponding to the secondary peak (i.e., at  $V_{helio} = 8345 \text{ km s}^{-1}$ . The  $V_{helio}$  of the spot is slightly different from  $V_{helio}$  of the main peak and secondary peak in the OH megamaser spectrum from the single-dish observations on account of velocity drift.) are distributed in two different rotating and expanding rings. This is consistent with our analysis of the single-dish observations and Model I.
2. The radii of the rotating and expanding rings, including the main and secondary peaks in Table 1 from the MERLIN observations and Model II, are very close to the results of the single-dish observations and Model I of a thin-disk NLR. The radial expansion velocity of the rings, including the main and secondary peaks, is consistent between Model I and Model II and the single-dish and MERLIN observations.

## References

- Baan, W. A., 1990, *ApJ*, 364, 65.  
 Baan, W. A., Haschick, A. D., & Henkel, C. 1989, *ApJ*, 346, 680.  
 Carroll, T. J., & Kwan, J. 1985, *ApJ*, 288, 73.  
 Chapman, J. M., et al. 1990, *MNRAS*, 244, 281.  
 Chevalier, R., & Clegg, A. 1985, *Nature*, 317, 44.  
 Harwit, M., et al. 1987, *ApJ*, 315, 28.  
 Montgomery, A. S., & Cohen, R. J. 1992, *MNRAS*, 254, 23P.  
 Staveley-Smith, L., et al. 1987, *MNRAS*, 226, 689.  
 Yu, Z.-Y. 1994, *Acta Ap. Sinica*, 14, 66.